Helium/H_2O_2 Atmospheric Pressure Plasma-Assisted Electrosurgery

Myeong Yeol Choi, Il Gyo Koo, Paul Y. Kim, Sung Kil Kang, Yoon-Sun Kim, Jae-Chul Jung, George J. Collins*

Electrosurgery (ES) is widely used by surgeons to dissect tissue and control bleeding. Electrosurgical devices achieve these effects through resistive heating of tissue that vaporizes cellular fluid to rupture cells and denatures proteins to produce a hemostatic coagulum. In this paper, the powered electrode of a 13.56 MHz atmospheric pressure plasma jet was employed in contact with tissue samples to vaporize or ablate tissue. In effect, monopolar ES was combined with plasma. We report both significantly higher tissue removal rate and lower electrical current flow through the tissue sample with plasma-assisted ablation compared to conventional electrosurgical ablation at the same generator output power.

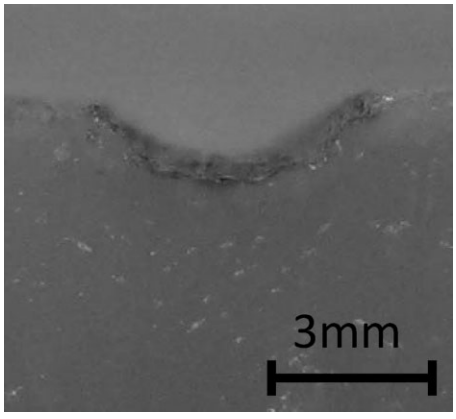

1. Introduction

Electricity has been used by surgeons to cut and coagulate tissues since the 1920s. Today, electrosurgery (ES) is one of the most common surgical techniques because the incisions can be performed faster with less blood loss compared to incisions made with a scalpel. A variety of surgical procedures employ ES including laparascopy,[1] arthroscopy,[2] otolaryngology,[3] and spine and cosmetic surgery.[4–6] In monopolar ES, high frequency electrical current is delivered to the tissue through an active electrode and returned to the generator through a dispersive electrode or pad to complete the circuit. The concentrated current density at the active electrode tip generates Joule heat, vaporizing intracellular water and rupturing cells, resulting in dissection.

M. Y. Choi, I. G. Koo, P. Y. Kim, S. K. Kang, Y.-S. Kim, J.-C. Jung, G. J. Collins
Department of Electrical and Computer Engineering, Colorado State University, Fort Collins, CO 80523, USA
E-mail: gcollins@engr.colostate.edu

Complications have been reported in ES, particularly with monopolar delivery. If the current is not sufficiently dispersed at the return pad, the energy may become focused in one area causing a burn. If the patient is improperly grounded, the current may follow an alternate ground path potentially leading to alternate-site burns to the patient or the surgeon.[7] The surgical effects of ES are based on heat hence there is inherent risk of thermal tissue injury. Thermal spread may damage vasculature, nerves, and other vital structures leading to delayed wound healing and increased postoperative pain.[8] Therefore, ES devices are faced with the challenge of hemostatic cutting with minimal tissue injury.

Monopolar ES can be augmented by adding argon gas flow in line with the active electrode. The resulting conductive plasma stream allows the current to arc from the electrode to the tissue without contact for hemostasis and tissue removal by vaporization, i.e., ablation. Recently we reported enhancement of non-contact tissue ablation by an RF-excited argon plasma jet through addition of chemical precursors to the argon stream.[9] Our current work was driven by the hypothesis that plasma chemical reactions could act synergistically with ES processes during

DOI: 10.1002/ppap.201200003

monopolar, contact mode tissue ablation. A synergistic effect would mean that less power and therefore less Joule heat may be required for tissue ablation, eventually leading to less thermal injury. In this paper, we report tissue ablation with a coaxial type helium/H_2O_2 plasma using a 13.56 MHz-powered electrode to deliver both plasma chemistry and electrical energy to the tissue sample.

2. Experimental Section

2.1. Atmospheric Pressure Plasma Generation

Figure 1a shows the coaxial plasma setup. The inner powered electrode consisted of an aluminum rod with a diameter of 3.1 mm. The outer grounded electrode consisted of an aluminum cylinder with inner and outer diameters of 5.6 and 6.3 mm, respectively. The powered electrode protruded 3 mm from the end of the grounded electrode. The powered electrode and inside wall of the grounded electrode were anodized with 16 and 40 μm thick nanoporous Al_2O_3, respectively.

Plasma was generated in the annulus as shown in Figure 1b, driven by 13.56 MHz RF power provided by a signal generator (N9310A, Agilent) and amplifier (SMZ-100, IFI). Helium was used as the discharge gas and the concentration of H_2O_2 in the plasma volume was controlled by adjusting helium gas flow through the H_2O_2 bubbler. The total helium flow rate was fixed at 600 sccm for optical emission spectroscopy and 1 000 sccm for all other studies by adding bypass flow to the flow through the bubbler.

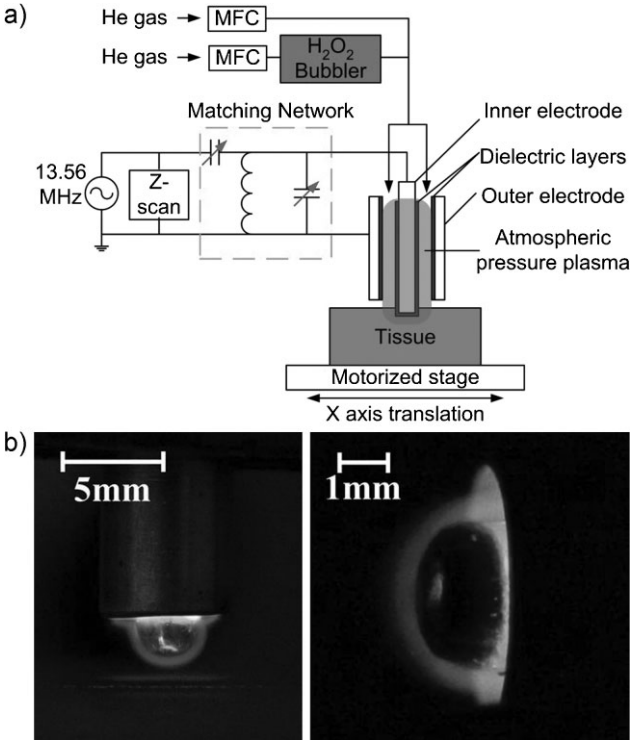

Figure 1. (a) Schematic of coaxial plasma experimental setup and (b) images of the plasma discharge (47 W, 1 000 sccm helium, 16 μl · min^{-1} H_2O_2).

2.2. Spectroscopic Diagnosis

The light emitted from the whole discharge region was delivered to a monochromator (SpectroPro®-2750, Princeton Instruments) coupled to a CCD camera (PIXIS-2K, Princeton Instruments) through a UV grade quartz focusing lens and an optical fiber. Absolute calibrations of the spectra were made using radiance standards including a calibrated mercury–argon lamp (HG-1, Ocean Optics). The spectra were normalized to the emission intensity of helium at 706 nm.

2.3. Electrical Characteristics Analysis

The plasma generating electrical system was controlled with careful measurement of forward, reflected, and delivered power, impedance, voltage, and current using a Z-scan (Advanced Energy) between the power supply and matching network. The voltages across the ES and plasma electrodes were measured with a high voltage probe (PPE6KV, Lecroy). The currents through the electrodes and the tissue samples were measured using a current transformer (CT-B2.5, Bergoz). The sample holder for measuring current through the tissue was made of copper metal and connected to the grounded electrode.

2.4. Tissue Preparation, Ablation and Characterization

Prepackaged retail chicken breast muscle portions were used to prepare samples approximately 2 cm × 2.5 cm in area, 1 cm in thickness, weighing 5 ± 1 g. Samples were placed on a stage at a fixed distance to form a 1 mm gap between the tissue and the grounded electrode when the protruding powered electrode was pressed into the tissue. Samples were scanned 25 mm long at 47 W RF power using a motorized linear stage at a rate of 10 mm · s^{-1}. A Force FX™ Electrosurgical Generator (Valleylab, Covidien) was employed for comparison with plasma. The ES electrode (E1550, Valleylab, Covidien) was selected on the basis of similar shape and tissue contact area to the plasma electrode. Samples were scanned by the ES electrode at 47 W similarly as described above for plasma. In both cases, the samples were weighed immediately before and after treatment using an analytical balance to determine the mass of removed tissue. Data are expressed as the mean ± SEM of 10 samples. Statistical analysis was performed using Student's *t*-test.

Following ablation by plasma or ES, samples were fixed in formalin, embedded in paraffin, serially sectioned, and stained with hematoxylin and eosin. The histological sections were examined with an Olympus BX52 light microscope and images were obtained with an Olympus DP70 digital camera.

Changes in the chemical composition of the tissue surface were determined by Fourier transform infrared (FTIR) spectroscopy. The samples were scanned 25 times at 4 cm^{-1} resolution using a single bounce Smart ITR for ATR (Attenuated Total Reflectance) with the FTIR system (Nicolet 6700, Thermofisher).

DOI: 10.1002/ppap.201200003

3. Results and Discussion

3.1. Generation and Characterization of Atmospheric Pressure Helium/H_2O_2 Plasma

Below 20 W, plasma discharge appeared to be homogeneous over the annular space between the electrodes. Discharge intensity increased with increasing power. Above 20 W, the discharge began to transition from α to γ mode producing strong emission in a semicircular region in addition to uniform and weak emission throughout the annulus. This transition from α to γ mode at 20 W was confirmed by measuring voltage and current as shown in Figure 2. In α mode, voltage and current increase as power increases. At 20 W, the voltage dropped and the discharge volume shrank resulting in γ mode, characterized by constant voltage and increasing current as power increases.[10] In addition, the glow plasma extended out around the protruding powered electrode with power over 20 W. Figure 3 shows representative optical emission spectra from helium and helium/H_2O_2 plasmas. The intensity of the OH band between 306 and 310 nm was increased in the emission spectrum of helium/H_2O_2 plasma compared to helium plasma under identical power and helium flow. This clearly demonstrates that H_2O_2 addition enhances OH radical generation. Helium plasma temperature, both with and without H_2O_2 addition, analyzed from emission spectrum was approximately 500 ± 50 K (230 ± 50 °C). Plasma electrode temperature measured by thermal IR camera was 210 °C.

3.2. Tissue Removal by Coaxial Plasma

When the powered electrode touched the tissue sample, the tissue acted as a ground path for electrical current, resulting in microdischarges between the electrode and the tissue surface. Hence in contact mode, this coaxial plasma combined plasma chemistry with RF voltage-driven discharges similar to the sparks observed in ES cutting. To better understand the effect of plasma chemistry in tissue ablation, helium plasma without H_2O_2 (47 W, 1 000 sccm helium) was applied to the tissue sample. The powered electrode immediately adhered to the tissue on contact and tissue ablation could not be achieved by translation of the motorized stage. In contrast, when the helium plasma was applied to the tissue sample under the same conditions but with the addition of 16 μl · min^{-1} H_2O_2, there was minimal adhesion and the tissue sample was ablated linearly using the motorized stage as shown in Figure 4. Although the plasma and electrode temperatures did not differ between helium and helium/H_2O_2 plasmas.

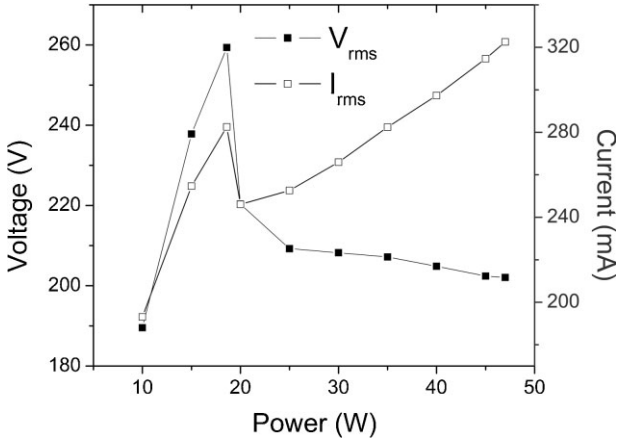

Figure 2. Voltage and Current versus Power of H_2O_2/He coaxial plasma (47 W, 1 000 sccm helium, 16 μl · min^{-1} H_2O_2).

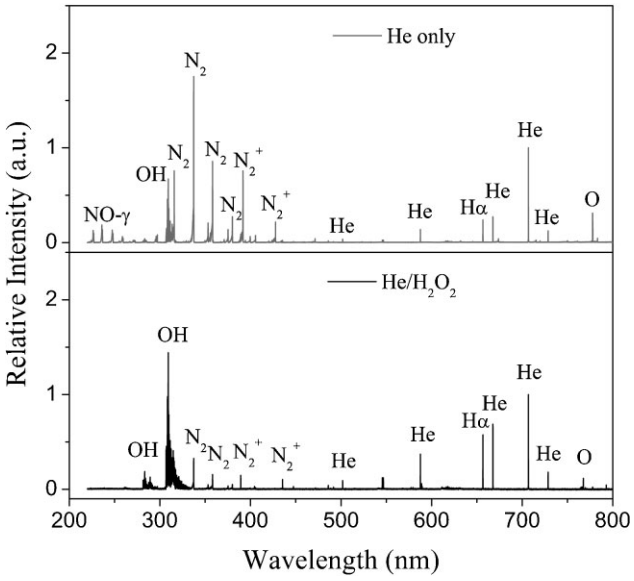

Figure 3. Typical optical emission spectra of helium and helium/H_2O_2 plasma discharges (47 W, 600 sccm helium, 16 μl · min^{-1} H_2O_2).

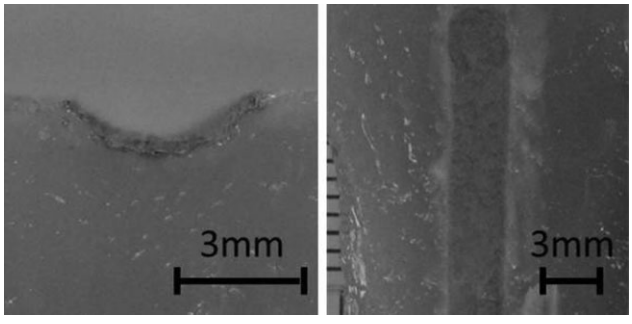

Figure 4. Side and top view of a chicken breast tissue sample treated by helium/H_2O_2 coaxial plasma (47 W, 1 000 sccm helium, 16 μl · min^{-1} H_2O_2, 10 mm · s^{-1} treatment speed).

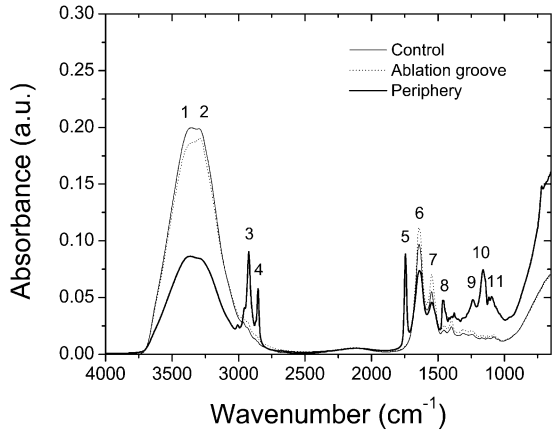

Figure 5. FTIR spectra of tissue samples treated by helium/H_2O_2 coaxial plasma (47 W, 1 000 sccm helium, 16 μl · min^{-1} H_2O_2, 10 mm · s^{-1} treatment speed) taken from areas inside the ablation groove (green) and from the immediate periphery (blue) compared to untreated tissue sample (black).

3.3. FTIR Analysis of Treated Tissue

Figure 5 shows representative FTIR spectra of control and helium/H_2O_2 plasma-treated tissues taken from areas inside the ablation groove and from the immediate periphery. A number of differences in the spectra are apparent in the periphery of the ablation groove as follows. The decrease in the relative intensity of the broad band centered around 3 339 cm^{-1} is attributed to a loss of water from the sample. Decreases in the relative intensities of bands assigned to amide I (1 658 cm^{-1}) and amide II (1 540 cm^{-1}) indicate a loss of protein secondary structure.[10,11] This protein denaturation was accompanied by considerable increases in the relative intensities of CH_2 (2 923, 2 853 and 1 451 cm^{-1}) and C=O (1 727–1 720 cm^{-1}) stretch assigned, respectively, to methylene and ester functional groups in lipids.[11,12] In addition, new peaks assigned to PO_2 (1 236 and 1 080 cm^{-1}) and C–O–C (1 170 cm^{-1}) stretch appear in the spectrum, which can be attributed primarily to nucleic acids and glycogen.[13] Interestingly, the spectrum of tissue inside the ablation groove did not differ markedly from control tissue. These results may be explained by the rupture of lipid membranes and forceful ejection of intracellular contents to the periphery as cells are vaporized during plasma treatment.

3.4. Comparison with Electrosurgery

To compare plasma ablation to ES ablation under similar conditions (47 W, 10 mm · s^{-1} treatment speed), an ES generator was employed with output current set to "cut" mode. The electrical current flow through the active electrodes and tissue samples during electrode–tissue contact are shown in Figure 6. The current through the

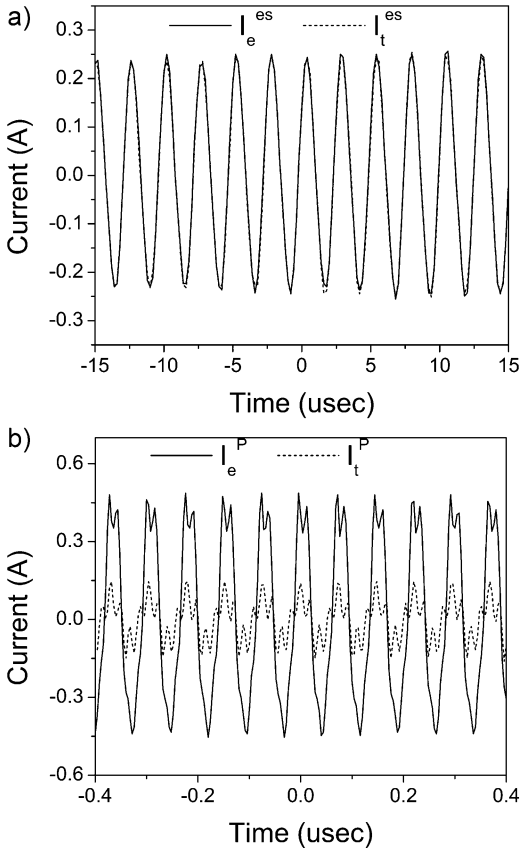

Figure 6. Electrical current flow through the active electrodes (I_e) and tissue samples (I_t) during (a) ES ablation and (b) plasma ablation.

tissue sample during ES ablation ($I_t^{es} = 167.2$ mA) was nearly equal to the current through the electrode ($I_e^{es} = 168.0$ mA). During plasma ablation, the current flow through the tissue sample ($I_t^{p} = 79.6$ mA) was significantly lower than the current flow through the electrode ($I_e^{p} = 322.8$ mA). A large portion of the delivered power was apparently consumed in the process of plasma generation.

Since the current flow through the tissue sample with ES was approximately twofold higher ($I_t^{es} \approx 2\, I_t^{p}$) than with plasma, the Joule heat generated in the tissue (P_t) was approximately fourfold greater ($P_t^{es} \approx 4\, P_t^{p}$). After accounting for tissue mass loss due to water evaporation induced by gas flow (5.16 ± 0.71 mg), the mass removed with plasma (29.44 ± 1.2 mg) and ES (26.3 ± 1.56 mg) in a 25 mm scan of the tissue sample were comparable (Figure 7). This data suggest that in addition to ES thermal ablation mechanisms based on Joule heat, plasma may provide other pathways for tissue removal. Histological sections of tissue samples after ES and helium/H_2O_2 plasma ablation showed that in both cases, the ablated surface is characterized by a layer of amorphous eosinophilic material with minimal carbonization or charring (Figure 8).

DOI: 10.1002/ppap.201200003

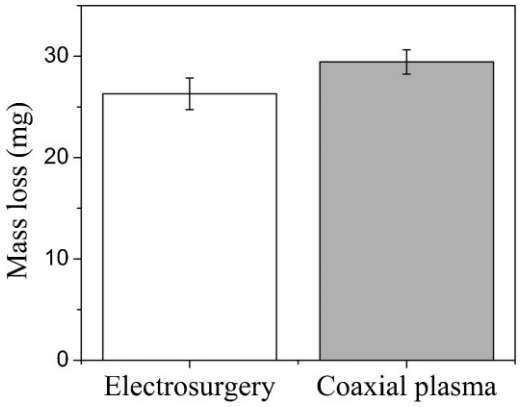

Figure 7. Tissue mass loss after 25 mm long ablation by ES (cut mode) and helium/H_2O_2 coaxial plasma (1 000 sccm helium, 16 $\mu l \cdot min^{-1}$ H_2O_2), both at 47 W and 10 $mm \cdot s^{-1}$ treatment speed.

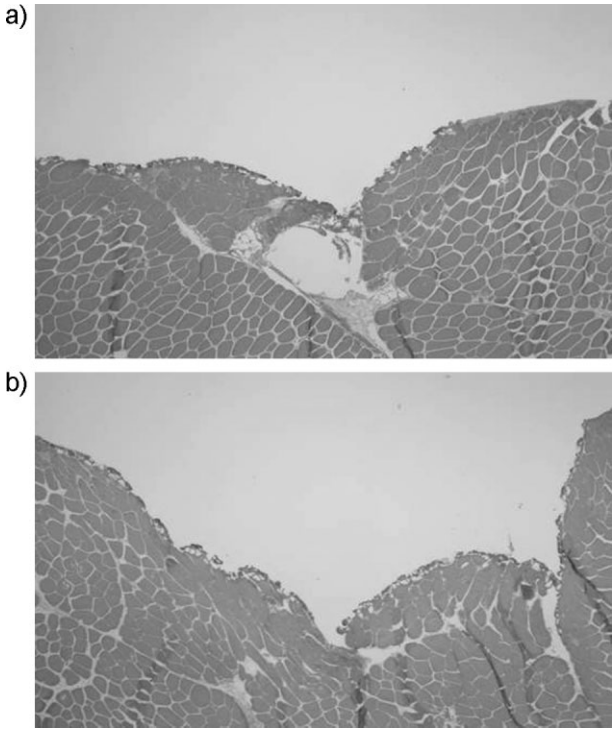

Figure 8. Histological sections of hematoxylin and eosin-stained tissue samples after treatment by (a) ES (cut mode) and (b) helium/H_2O_2 plasma (1 000 sccm helium, 16 $\mu l \cdot min^{-1}$ H_2O_2), both at 47 W and 10 $mm \cdot s^{-1}$ treatment speed.

4. Conclusion

In summary, γ mode discharge of RF plasma was employed as a monopolar contact electrode to enhance ES ablation. The addition of H_2O_2 into the helium plasma was found to increase the concentration of chemically reactive OH species (Figure 3). This eliminated tissue adhesion to the powered electrode through an as yet undetermined mechanism. Although the helium and helium/H_2O_2 plasma and electrode temperatures did not differ, tissue ablation only occurred with the addition of H_2O_2 under our experimental conditions. At 47 W input power, helium/H_2O_2 plasma removed tissue at a rate comparable to ES, but with less electrical current flow through the tissue. Taken together, these results suggest a possible role of plasma chemistry in the ablation process that may allow for desired surgical effects at lower power and lead to decreased risk of thermal injury and other adverse effects of electrical current flow through a patient.

Acknowledgements: The work herein was funded by Covidien Ltd.

Received: January 10, 2012; Revised: May 13, 2012; Accepted: June 11, 2012; DOI: 10.1002/ppap.201200003

Keywords: ablation; atmospheric pressure glow discharges (APGD); electrosurgery

[1] M.-P. Wu, C.-S. Ou, S.-L. Chen, E. Y. T. Yen, R. Rowbotham, *Am. J. Surg.* **2000**, *179*, 67.
[2] J. D. Polousky, T. P. Hedman, C. T. Vangsness, Jr., *Arthroscopy* **2000**, *16*, 813.
[3] J. Woloszko, M. Kwende, K. R. Stalder, *Proc. SPIE* **2003**, *4949*, 341.
[4] E. W. Elliott-Lewis, J. Jolette, J. Ramos, *Neurosurgery* **2010**, *67*, 166.
[5] A. J. Burns, S. G. Holden, *Lasers Surg. Med.* **2006**, *38*, 575.
[6] E. P. Tierney, C. W. Hanke, *Dermatol. Surg.* **2009**, *35*, 1324.
[7] N. N. Massarweh, N. Cosgriff, D. P. Slakey, *J. Am. Coll. Surg.* **2006**, *202*, 520.
[8] M. K. Flynn, A. C. Weidner, C. L. Amundsen, *Am. J. Obstet. Gynecol.* **2006**, *195*, 1869.
[9] I. G. Koo, C. A. Moore, M. Y. Choi, G. J. Kim, P. Y. Kim, Y. S. Kim, Z. Yu, G. J. Collins, *Plasma Process. Polym.* **2011**, *8*, 1103.
[10] S. Y. Moon, J. K. Rhee, D. B. Kim, W. Choe, *Appl. Phys. Lett.* **2006**, *13*, 033502.
[11] H. Susi, D. M. Byler, *Methods Enzymol.* **1986**, *130*, 290.
[12] S. Krimm, J. Bandekar, *Adv. Protein Chem.* **1986**, *38*, 181.
[13] O. Bozkurt, M. D. Bilgin, F. Severcan, *Spectroscopy* **2007**, *21*, 151.